Use of D-STATCOM for Solid State LED Lamp Harmonic Power Mitigation

Wesam Rohouma
Electrical Engineering Department
College of EngineeringTechnology & Industrial Trades
University of Doha for Science & Technology
Doha, Qatar
wesam.rohouma@ieee.org

Robert S. Balog
Renewable Energy & Advanced Power Electronics Research Laboratory
Texas A&M University at Qatar
Doha, Qatar
robert.balog@ieee.org

Miroslav M. Begovic
Department of Electrical & Computer Engineering
Texas A&M University at Qatar
College Station, Texas USA
begovic@tamu.edu

Aaqib Ahmad Peerzada
Department of Electrical & Computer Engineering
Texas A&M University at Qatar
College Station, Texas USA
peerzada@tamu.edu

***Abstract* — The use of light-emitting diode (LED) lamps is increasing dramatically in many countries, spurred by energy conservation initiatives. Some countries have gone as far as to completely ban the old incandescent lightbulbs in favour of the more efficient LEDs. However, many of these LED lamps, particularly low-cost and non-dimmable models, act as non-linear loads in the electrical power system, drawing non-sinusoidal current due to the power electronic components inside them to provide the required rectified and regulated direct current (DC). Thus, while solid-state lightbulbs help in energy conservation, they can have the unintended consequence of lowering the power quality in the smartgrid electrical distribution network. In this paper, a matrix converter topology based distribution static synchronous compensators (D-STATCOM) is proposed for use in the low voltage distribution network to compensate the harmonics generated from the LED lamps. The D-STATCOM is controlled using a finite control set model predictive control (FCS-MPC). Experimental studies were performed, and the results obtained showed the effectiveness of the proposed technology in harmonics power mitigation.**

Keywords— Solid-state LED lamps, D-STATCOM, Harmonics power mitigation, Model Predictive Control, Matrix Converter

I. INTRODUCTION

Lighting account for nearly 20% of the world's electricity consumption [1]. Energy-saving LED lamps offer around 65% reduction in electricity demand compared with the traditional incandescent lamps for the same luminous flux [2, 3]. In many countries, the use of energy-efficient LED lamps continues to increase not only with the energy conservation driver but with for the laws applied in many countries to ban the use of incandescent lamps [4]. On the other hand, the operation of the solid states LED lamps require power electronic drivers to convert the AC to DC and perform power factor correction, which inherently has non-linear characteristics. LED lamps draw significant non-sinusoidal current and produce harmonics pollution in distribution network [4, 5]. The negative effects of harmonics on power system components and user equipment are well studied in the literature [6].

In this regard, there is a pressing need to mitigate this harmonic pollution locally near its source. D-STATCOM and shunt active power filters (SAPF) are the most dominant technology available for power quality and harmonic power mitigation in distribution networks. Typically, the D-STATCOM and the SAPF topology is based on the voltage source converter (VSC) [7, 8] which make use of electrolytic capacitors (e-caps) to stores the energy needed. However, e-caps have well-known failure modes and have been shown to exhibit accelerated wear and tear in hot climatic conditions. Failure types of DC capacitors are presented in [9] with an estimated 30% of power electronics failures occurring mainly because of the capacitors [10, 11]. In order to overcome the well-known failure modes of the existing VSC topologies, a matrix converter (MC) based capacitor-less D-STATCOM is proposed as a good alternative to replace the standard VSC topology [12-22].

In this paper, a capacitor-less D-STATCOM based matrix converter, as shown in Fig.1 will be used to provide the required harmonics mitigation in the distribution network. Experimental results will be presented using 7.5 kVA experimental prototype.

II. SYSTEM STRUCTURE

Typical distribution system network consists of number of loads connected at the medium and low voltage sides. At the low voltage network, a large number of loads including non-linear loads (solid states LED lamps) and linear inductive

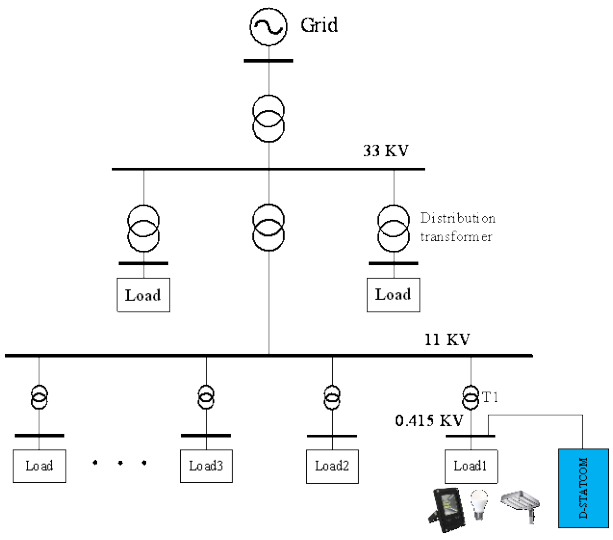

Fig. 1. Distribution system one-line diagram showing the hierarchy of voltages from sub-transmission down to the load. The D-STATCOM is shunt-connected at a specific bus in the distribution network.

XXX-X-XXXX-XXXX-X/XX/$XX.00 ©20XX IEEE

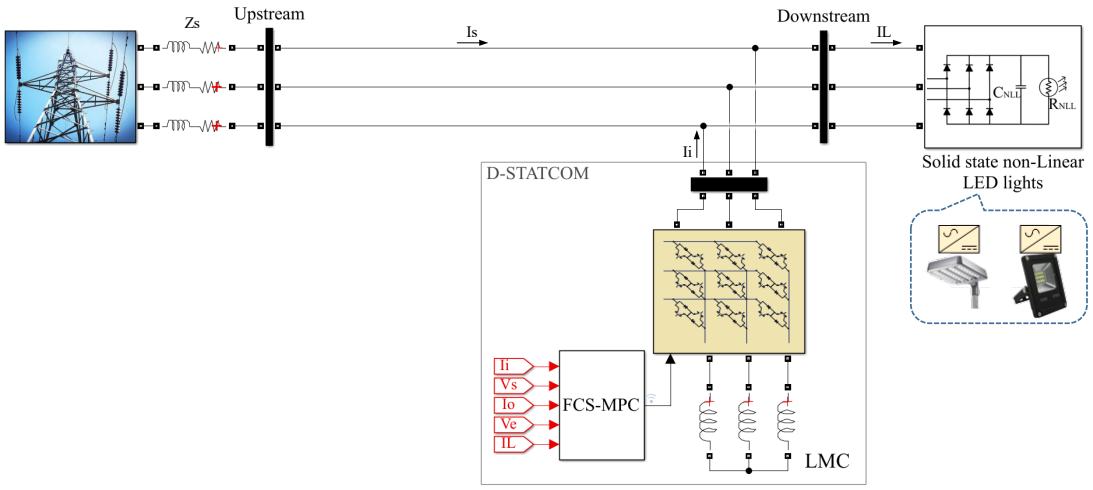

Fig. 2. Model of the radial distribution network at the connection bus for the D-STATCOM. The upstream refers to moving in the direction toward the distribution transformer and downstream refers to moving away from the distribution transformer.

loads connected at different locations via distribution transformer as shown in Fig. 1. To mitigate the harmonics and other power quality issues, D-STATCOM based matrix converter is connected at the PCC near the point of load connection as in the figure below. The aggregate behaviours of the solid-state LED lamps are represented as full-wave three-phase bridge rectifier as in Fig. 2. The D-STATCOM system is based on direct matrix converter with inductive energy storage connected at the output side of the converter.

A. Load model

The share of non-linear loads in the distribution network has increased dramatically due to the increasing adoption of power-electronics enabled devices in commercial and residential sectors. The loads in the low voltage distribution network consist of linear loads and a significant percentage of non-linear loads that include LED lights. In this paper, the worst-case scenario is considered in which 100% of the loads are non-linear on the distribution feeder, and this scenario is used here to evaluate the performance of the D-STATCOM under this high-penetration condition. The aggregate behavior of the non-linear loads can be represented by a three-phase diode bridge rectifier with DC voltage capacitors and resistors.

B. D-STATCOM model

Three-phase MC is the main building block in the proposed D-STATCOM. It consists of a matrix converter with inductive energy storage controlled using dSPACE platform based on MPC control strategy.

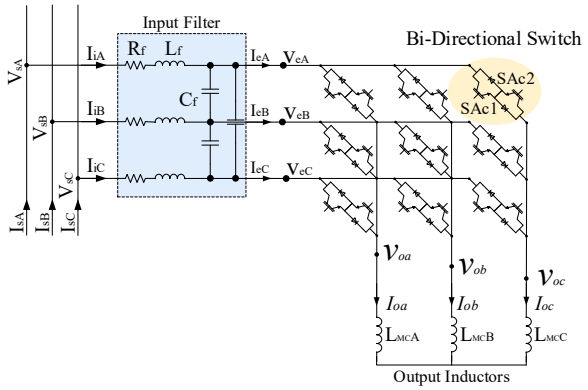

Fig. 3. Power converter power topology showing the 3x3 direct matrix converter with inductive load (LMC). Since there is no dc link, there are no dc bus capacitors to wear out and fail.

1) Matrix converter model

The direct matrix converter system used in this application consists of topology depicted in Fig. 3. the MC power board consists of an array of nine bidirectional switches each switch comprised of two IGBT parallel diode pairs connected in the anti-parallel configuration. The MC is connected to the network bus through an input filter L_f, C_f, R_f. This filter is used to eliminate high-frequency harmonics from propagating to the rest of the network. The output voltages and input currents of the MC were calculated according to (1), (2) and (3) as a function of MC input voltages, output currents and the switching function. The inductive load constrains the switching to avoid interruption of MC output current. The voltage-source input constrains the switching to avoid shorting the input phases.

$$S_{Ay}+S_{By}+S_{Cy}=1 \quad \text{where} \quad y \in (a,b,c) \tag{1}$$

$$\begin{bmatrix} v_{oa} \\ v_{ob} \\ v_{oc} \end{bmatrix} = \begin{bmatrix} S_{Aa} & S_{Ba} & S_{Ca} \\ S_{Ab} & S_{Bb} & S_{Cb} \\ S_{Ac} & S_{Bc} & S_{Cc} \end{bmatrix} . \begin{bmatrix} V_{SA} \\ V_{SB} \\ V_{SC} \end{bmatrix} \tag{2}$$

$$\begin{bmatrix} I_{inA} \\ I_{inB} \\ I_{inC} \end{bmatrix} = \begin{bmatrix} S_{Aa} & S_{Ab} & S_{Ac} \\ S_{Ba} & S_{Bb} & S_{Bc} \\ S_{Ca} & S_{Cb} & S_{Cc} \end{bmatrix} . \begin{bmatrix} I_{oa} \\ I_{ob} \\ I_{oc} \end{bmatrix} \tag{3}$$

where $V_{oa}(t)$, $V_{ob}(t)$ and $V_{oc}(t)$, $I_{oa}(t)$, $I_{ob}(t)$ and $I_{oc}(t)$ are the output voltages and currents of the matrix converter respectively. While, $V_{SA}(t)$, $V_{SB}(t)$ and $V_{SC}(t)$, $I_{iA}(t)$, $I_{iB}(t)$ and $I_{iC}(t)$ are the input voltages and currents of the matrix converter, and $S_{ij}(t)$ is the switching function with $i=A,B,C$, and $j=a,b,c$. Proper choice of S will lead to a phase-reversal of the current so that the inductive load appears capacitive at the input to the MC to supply reactive power to the network [13, 14, 23].

C. D-STATCOM Control

FCS-MPC is used to control the converter to provide the required power quality mitigation. There are several control schemes reported in the literature to control the MC, including, repetitive control, resonant, proportional-integral

(PI) control, and model predictive control [14, 24-30]. Research results show that MPC is the most promising alternative due to its simplicity and flexibility to include additional terms in the controller and prioritise there relative importance using weight factors [30]. The controller starts with reference current generation then model predictive control to track the reference currents.

1) Reference current detection:

For reference current detection the synchronous rotating reference frame (SRF) are most widely used and it has been adopted in this paper [31]. In this step, the load currents and voltages are measured, filtered, and reference currents are extracted according to the synchronous reference frame (SRF) method. SRF theory is based on the transformation of currents in synchronously rotating *d–q* frame [32, 33]. The transformation to the *d-q* reference frame from the ABC reference frame is given as

$$\begin{bmatrix} \mathrm{Id} \\ \mathrm{Iq} \\ \mathrm{I0} \end{bmatrix} = \sqrt{\frac{2}{3}} \begin{bmatrix} \cos(\omega t) & \cos(\omega t - 2\pi/3) & (\omega t + 2\pi/3) \\ -\sin(\omega t) & -\sin(\omega t - 2\pi/3) & -\sin(\omega t + 2\pi/3) \\ 1/\sqrt{2} & 1/\sqrt{2} & 1/\sqrt{2} \end{bmatrix} \cdot \begin{bmatrix} \mathrm{I_{LA}} \\ \mathrm{I_{LB}} \\ \mathrm{I_{LC}} \end{bmatrix} \quad (4)$$

The block diagram of the SRF method is shown in Fig. 4. The three-phase load current is measured then transformed to the *dq0* reference frame to extract the active and reactive current components of the load current; the new components consist of DC part that represents the fundamental component of the current and the AC part that represent the harmonics. Using a high pass filter (HPF), the harmonic component can be extracted and then transformed back to the ABC reference frame to be used as a reference current for the controller.

2) Finite control set model predictive control

The structure of the FCS-MPC used in this paper is shown in Fig.5. The voltage at PCC $V_S(k)$, the input current of MC $I_i(k)$, the input voltage of MC $V_e(k)$ and the output current $I_o(k)$ are measured in each sampling period. These values are used to predict the future values of the input current $I_i(k+1)$ and output currents $I_o(k+1)$. Using the model of the MC, the controller will predict all the values of the input and output current for each switching state and select the state that returns the minimum value of the cost function (J). In order to predict the output currents of the MC, the model for the MC output inductors is derived as

$$L_{MC}\frac{di_o(t)}{dt} = v_o(t) - R_{LMC}i_o(t) \quad (5)$$

The derivative in (5) is approximated using the forward Euler method for each k^{th} discrete sample time steps:

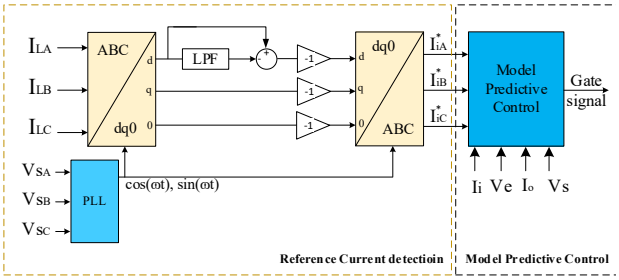

Fig. 4. Reference current detection based on SRF.

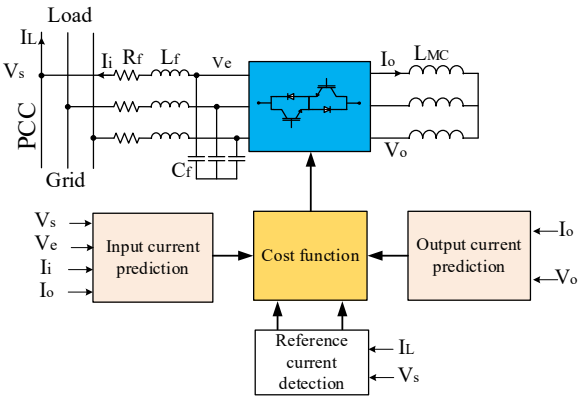

Fig. 5. Finite control set model predictive control (FCS-MPC) block diagram.

$$\frac{di_o(t)}{dt} \approx \frac{i_o(k+1) - i_o(k)}{T_S} \quad (6)$$

From (5) and (6), the discrete-time model estimates the current at the next sample (k+1) is given as [34]:

$$i_o^p(k+1) = \left(1 - \frac{R_{LMC}T_s}{L_{MC}}\right) i_o(k) + \frac{T_s}{L_{MC}} v_{oLN}(k) \quad (7)$$

The input filter model as shown in fig. 1, can be represented by following continuous-time equations:

$$v_s(t) = R_f i_i(t) + L_f \frac{d}{dt} i_i(t) + V_e(t) \quad (8)$$

$$i_i(t) = i_e(t) + C_f \frac{d}{dt} V_e(t) \quad (9)$$

where v_s, v_e are the input and output voltages of the filter and i_{in} and i_e are the input and output currents of the filter. The state-space model of the filter can be written as

$$\begin{bmatrix} V_e^*(t) \\ i_i^*(t) \end{bmatrix} = A \begin{bmatrix} V_e(t) \\ i_i(t) \end{bmatrix} + B \begin{bmatrix} V_s(t) \\ i_e(t) \end{bmatrix} \quad (10)$$

Adding the coefficient of the system matrices results in

$$\begin{bmatrix} V_e^*(t) \\ i_i^*(t) \end{bmatrix} == \underbrace{\begin{bmatrix} 0 & \frac{1}{C_f} \\ -\frac{1}{L_f} & -\frac{R_f}{L_f} \end{bmatrix}}_{A_c} \begin{bmatrix} V_e(t) \\ i_i(t) \end{bmatrix} + \underbrace{\begin{bmatrix} 0 & -\frac{1}{C_f} \\ \frac{1}{L_f} & 0 \end{bmatrix}}_{B_c} \begin{bmatrix} Vs(t) \\ i_e(t) \end{bmatrix} \quad (11)$$

Finally, the discrete model of the input filter using zero-order hold and sample time T_s is given by [34]

$$\begin{bmatrix} V_e(k+1) \\ i_i(k+1) \end{bmatrix} + A_q \begin{bmatrix} V_e(k) \\ i_i(k) \end{bmatrix} + B_q \begin{bmatrix} V_s(k) \\ i_e(k) \end{bmatrix} \quad (12)$$

where

$$A_q = e^{A_c T_s} \text{ and } B_q = \int_0^{T_s} e^{A_c(T_s - \tau)} B_c d\tau \quad (13)$$

Finally, the discrete-time form of the input currents for a sampling time T_s can be written as [34]

$$\begin{aligned} i_i^p(k+1) = {} & A_{q(2,1)} V_e(k) + A_{q(2,2)} I_i(k) \\ & + B_{q(2,1)} V_s(k) + B_{q(2,2)} I_e(k) \end{aligned} \quad (14)$$

The cost function can be written as

$$J = \lambda_1 \left(\left| I_{i\alpha}^{p} - i_{i\alpha}^{*} \right| + \left| I_{i\beta}^{p} - i_{i\beta}^{*} \right| \right) + \lambda_2 \left(\left| I_{o\alpha}^{p} - i_{o\alpha}^{*} \right| + \left| I_{o\beta}^{p} - i_{o\beta}^{*} \right| \right) \quad (15)$$

where J is the cost function and $I_{i\alpha}$ and $I_{i\beta}$ are the MC input currents, $I_{o\alpha}$, $I_{o\beta}$ is the MC output currents. The weight factors λ_1, λ_2 are adjusted to priorities the different parts of the cost function. Optimal tuning of these weight factor is still an open topic for research [35, 36]. In this paper, manual tuning is performed according to the guidelines from [36].

III. EXPERIMENTAL RESULTS

To verify the harmonics compensation capability of the capacitor-less D-STATCOM, a hardware testbed and D-STATCOM converter, shown in Fig.6, was developed to test the system in Fig. 2. System parameters are provided in Table I. The testbed consists of an upstream side (12 kVA three-phase grid simulator NHR-9410), a downstream side (electronic load from Cenergia), D-STATCOM unit (7.5 kVA matrix converter unit with three-phase inductors connected at its the output side), and control platform (dSPACE Scalexio) to control the matrix converter.

TABLE I. SYSTEM PARAMETERS

PARAMETER	VALUE
Voltage, V_{LL}	415V
Frequency	50Hz
Source impedance (Ls)	1mH
Three-phase bridge rectifier DC capacitor (C_NLL)	40uF
Three-phase bridge rectifier resistor (R_NLL)	125 Ohm
Output chokes inductance L_{MC}	36mH
Input filter resistance Rf	1 Ω
Input filter inductance Lf	2.5mH
Input filter capacitor Cf/phase	12 uF
Sampling time Ts	40µs
Weight factor λ1	1
Weight factor λ2	0.1

The matrix converter unit consists of nine IGBT modules SK60GM123, isolated gate drive circuits, current direction detection circuit, clamp circuit for overvoltage protection, voltage transducers LEM LV 25-p and current transducers LEM LP 55. The dSPACE control platform consists of a processing unit and LabBox™ with 4 FPGA modules each

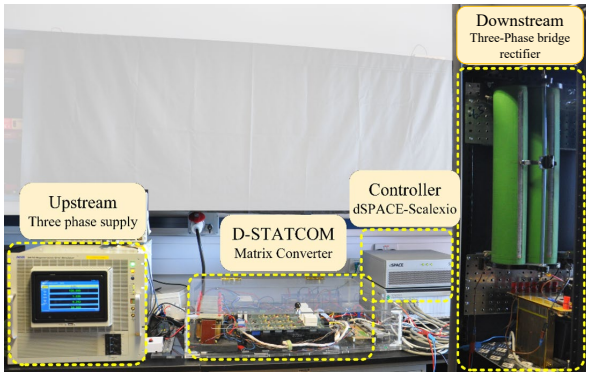

Fig. 10. Experimental setup of 7.5kVA D-STATCOM.

module has 5 ADC 14bit resolution, 10 digital I/O pins and 5 analogue output pins. The MPC strategy is implemented in dSPACE Scalexio processing unit, while the measurements and four-step commutation and protection are implemented in dSPACE LabBox™ unit. dSPACE ControlDesk™ software is

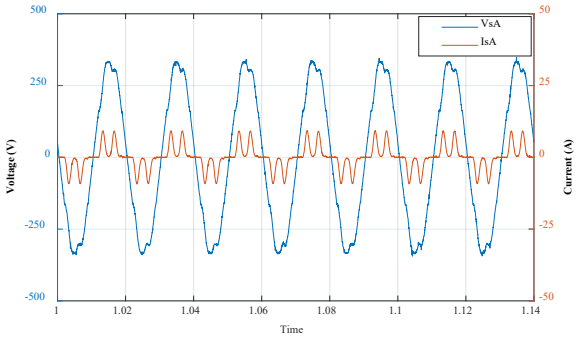

Fig. 6. Experimental results of upstream phase voltage (V_{sA}) and current (I_{sA}) before compensation.

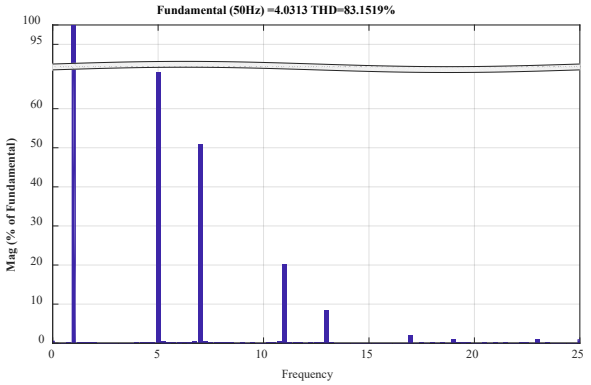

Fig. 7. Experimental results showing source current (I_{sA}) spectra before compensation.

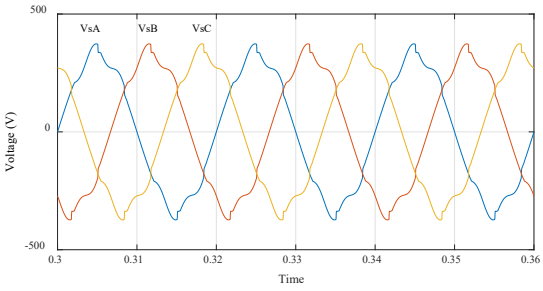

Fig. 8. Experimental results showing three phase voltages at PCC before compensation.

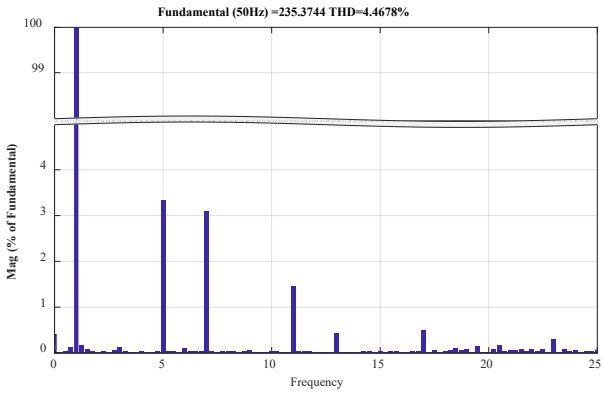

Fig. 9. Experimental results showing source voltage (V_{sA}) spectra before compensation.

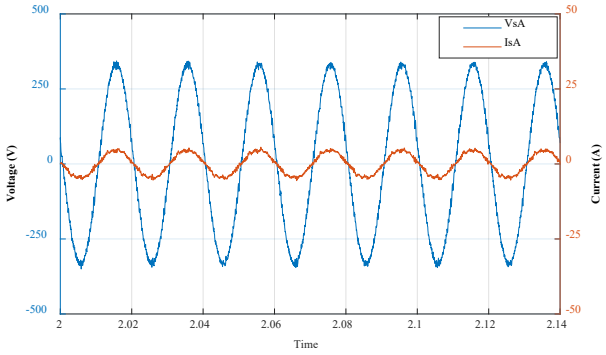

Fig. 12. Experimental results of upstream phase voltage (V_{sA}) and current (I_{sA}) after compensation.

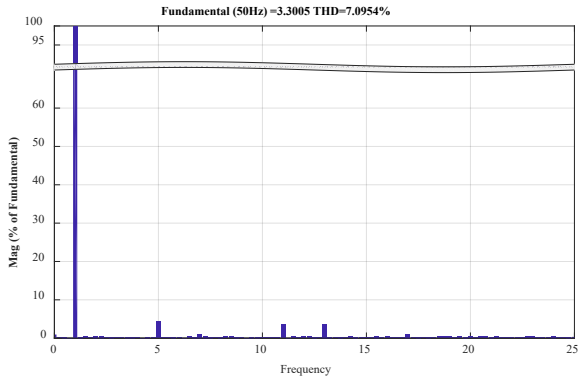

Fig. 13 Experimental results showing source current (I_{sA}) spectra after compensation.

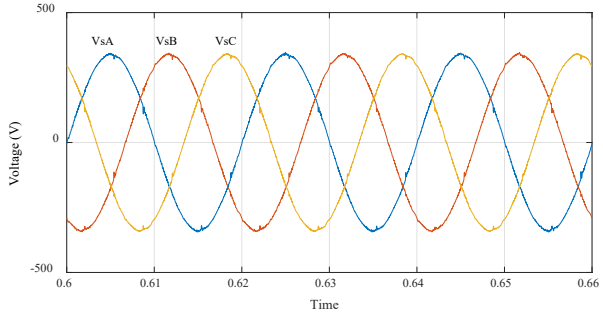

Fig. 14. Experimental results showing three phase voltages at PCC after compensation.

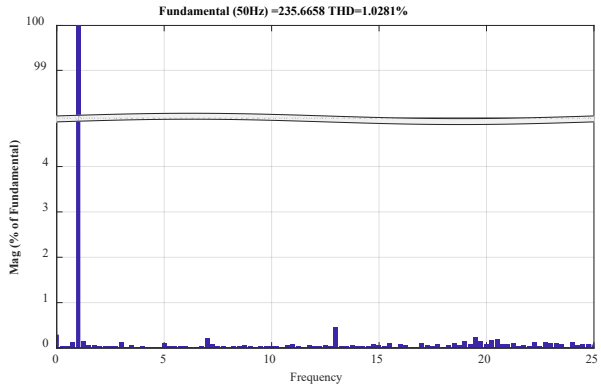

Fig. 15. Experimental results showing source voltage (V_{sA}) spectra after compensation.

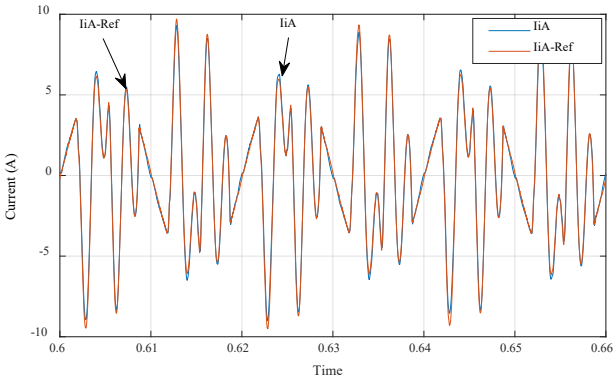

Fig. 11. Experimental results showing the input current (I_{iA}) tracking the reference ($I_{iA\text{-}Ref}$) using MPC after compensation.

used to supervise and control the experiment in real-time and view and store the experimental results and modify the desired control parameters during the experiment.

Initially, the LED load is connected to the grid-simulator source, and the performance of the system without the D-STATCOM is determined. Fig. 7 shows the experimental results of the supply voltage and current of phase (A) measured in volt and ampere respectively. Initially, it can be seen that the source current is distorted with total harmonics distortion (THD) of 83.1% as can be seen in Fig.8. The distorted source current interact with the series source impedance and negatively affect the source voltage as can be seen in Fig.9. Spectrum analysis of upstream voltage is shown in Fig.10 with THD of 4.4%. After the D-STATCOM is connected to the PCC, Fig. 11 shows the source voltage and current, and it can be noted that the source current becomes sinusoidal with THD of 7% as can be observed in spectrum analysis in Fig.12. After connecting the D-STATCOM to the system the three-phase source voltage looks sinusoidal with low distortion of 1% as in Fig.13 and Fig.14. D-STATCOM input current waveforms compared with the reference is shown in Fig. 15. It can be seen that after D-SATCOM is connected the controller was able to control the converter and achieve good tracking of the input currents of the converter.

IV. CONCLUSION

In this paper, the performance of capacitor-less D-STATCOM controlled using FCS-MPC is presented for harmonics compensation due to the increased use of non-linear solid-state LED lights in low voltage distribution network. FCS-MPC is used to control the proposed converter, and synchronous reference frame method is adapted to generate the reference current for the MPC. Results from the 7.5kVA experimental setup show that the proposed shunt connected D-STATCOM is able to provide good harmonics mitigation even with large integration of non-linear solid states lights in low voltage network.

ACKNOWLEDGEMENT

This publication was made possible by NPRP grant # 13S-0213-200357 from the Qatar National Research Fund (a member of Qatar Foundation). The statements made herein are solely the responsibility of the authors.

The authors acknowledge and thank Professor Pat Wheeler and Professor Lee Empringham from the power

electronics and machine control group at the University of Nottingham, UK, for their collaboration on the matrix converter prototype design and fabrication.

REFERENCES

[1] S. T. Tan, X. W. Sun, H. V. Demir, and S. P. DenBaars, "Advances in the LED Materials and Architectures for Energy-Saving Solid-State Lighting Toward "Lighting Revolution"," *IEEE Photonics Journal*, vol. 4, no. 2, pp. 613-619, April 2012.

[2] H. Shabbir, M. U. Rehman, S. A. Rehman, S. K. Sheikh, N. Zaffar, H. Shabbir, M. U. Rehman, S. A. Rehman, S. K. Sheikh, and N. Zaffar, "Assessment of harmonic pollution by LED lamps in power systems," in *IEEE Clemson University Power Systems Conference*, 11-14 March 2014 pp. 1-7.

[3] V. Ćuk, J. F. G. Cobben, W. L. Kling, and R. B. Timens, "An analysis of diversity factors applied to harmonic emission limits for energy saving lamps," in *Proceedings of 14th International Conference on Harmonics and Quality of Power - ICHQP 2010*, 26-29 Sept. 2010, pp. 1-6.

[4] A. M. Blanco, R. Stiegler, and J. Meyer, "Power quality disturbances caused by modern lighting equipment (CFL and LED)," in *2013 IEEE Grenoble Conference*, 16-20 June 2013, pp. 1-6.

[5] M. M. U. Rehman, H. Shabbir, S. A. Rehman, S. K. Sheikh, and N. Zaffar, "A Comparative Analysis of Electrical and Photo Characteristics of LED Lights," in *10th International Conference on Frontiers of Information Technology*, 17-19 Dec. 2012, pp. 219-224.

[6] V. E. Wagner, J. C. Balda, D. C. Griffith, A. McEachern, T. M. Barnes, D. P. Hartmann, D. J. Phileggi, A. E. Emannuel, W. F. Horton, W. E. Reid, R. J. Ferraro, and W. T. Jewell, "Effects of Harmonics on Equipment," *IEEE Transactions on Power Delivery*, vol. 8, no. 2, pp. 672-680, April 1993.

[7] J. Dixon, L. Moran, J. Rodriguez, and R. Domke, "Reactive power compensation technologies: State-of-the-art review," *Proceedings of the IEEE*, vol. 93, no. 12, pp. 2144-2164.

[8] F. Shahnia, S. Rajakaruna, and A. Ghosh, "Static Compensators (STATCOMs) in Power Systems," in *Power Systems*: Springer, 2015.

[9] A. S. Farag, C. Wang, T. C. Cheng, G. Zheng, Y. Du, L. Hu, B. Palk, and M. Moon, "Failure analysis of composite dielectric of power capacitors in distribution systems," *IEEE Transactions on Dielectrics and Electrical Insulation*, vol. 5, no. 4, pp. 583-588, Aug 1998.

[10] T. Orłowska-Kowalska, F. Blaabjerg, and J. Rodríguez, *Advanced and Intelligent Control in Power Electronics and Drives.* vol. 531: Springer, 2014.

[11] S. Yang, A. Bryant, P. Mawby, D. Xiang, L. Ran, and P. Tavner, "An Industry-Based Survey of Reliability in Power Electronic Converters," *IEEE Transactions on Industry Applications*, vol. 47, no. 3, pp. 1441-1451, May-June 2011.

[12] W. Rohouma, R. S. Balog, A. A. Peerzada, and M. M. Begovic, "D-STATCOM for a Distribution Network with Distributed PV Generation," presented at *IEEE 2018 International Conference on Photovoltaic Science and Technologies (PVCON)*, 4-6 July 2018.

[13] W. Rohouma, R. S. Balog, A. A. Peerzada, and M. M. Begovic, "Capacitor-Less D-STATCOM for Reactive Power Compensation," presented at *IEEE 12th International Conference on Compatibility, Power Electronics and Power Engineering (CPE-POWERENG 2018)*, 10-12 April 2018.

[14] M. B. Shadmand, M. Mosa, R. S. Balog, and H. Abu-Rub, "Model Predictive Control of a Capacitorless Matrix Converter-Based STATCOM," *IEEE Journal of Emerging and Selected Topics in Power Electronics*, vol. 5, no. 2, pp. 796-808, June 2017.

[15] D. Balakrishnan and R. S. Balog, "Capacitor-less VAR compensator based on matrix converter," presented at *IEEE North American Power Symposium (NAPS)*, 26-28 Sept. 2010.

[16] P. Zanchetta, P. Wheeler, L. Empringham, and J. Clare, "Design control and implementation of a three-phase utility power supply based on the matrix converter," *IET Power Electronics*, vol. Volume 2, no. Issue 2, pp. 156 - 162, March 2009.

[17] W. Rohouma, R. S. Balog, A. A. Peerzada, and M. M. Begovic, "Fault Tolerant D-STATCOM based Matrix Converter," in *IEEE 2nd International Conference on Smart Grid and Renewable Energy (SGRE)*, Doha, QATAR, 19-21 November 2019, pp. 1-6.

[18] W. Rohouma, R. S. Balog, A. A. Peerzada, and M. M. Begovic, "Parallel Operation of Capacitor-less D-STATCOM to Allow More Penetration of Photovoltaic Systems in Distribution Network," in *IEEE 47th IEEE Photovoltaic Specialists Conference (PVSC)*, 15 June - 21 August 2020, pp. 2777-2782.

[19] W. Rohouma, R. S. Balog, and H. Zubi, "Application of a Capacitor-Less D-STATCOM for Power Quality Enhancement in a Typical Telecom Data Center," in *IEEE 3rd International Conference on Smart Grid and Renewable Energy (SGRE'22)*, Doha, QATAR, 20-22 March 2022, pp. 1-6.

[20] W. Rohouma, M. Metry, R. S. Balog, A. A. Peerzada, and M. M. Begovic, "Adaptive Model Predictive Controller to Reduce Switching Losses for a Capacitor-Less D-STATCOM," *IEEE Open Journal of Power Electronics (OJ-PEL)*, vol. 1, pp. 300-311, 2020.

[21] W. Rohouma, M. Metry, R. S. Balog, A. A. Peerzada, M. Begovic, and Z. Dao, "Analysis of the Capacitor-Less D-STATCOM for Voltage Profile Improvement in Distribution Network With High PV Penetration," *IEEE Open Journal of Power Electronics (OJ-PEL)*, vol. 3, pp. 255-270, 2022.

[22] W. Rohouma, R. S. Balog, A. A. Peerzada, and M. M. Begovic, "Development of a Capacitor-less D-STATCOM for Power Quality Improvement in Low Voltage Network," in *IEEE 13th International Conference on Compatibility, Power Electronics and Power Engineering (CPE-POWERENG)*, Sønderborg, DENMARK, 23-25 April 2019.

[23] W. M. Rohouma, L. d. Lillo, S. López, P. Zanchetta, and P. W. Wheeler, "A single loop repetitive voltage controller for a four legs matrix converter ground power unit," in *IEEE Proceedings of the 14th European Conference on Power Electronics and Applications*, 30 Aug.-1 Sept. 2011, pp. 1-9.

[24] W. Rohouma, P. Zanchetta, P. W. Wheeler, and L. Empringham, "A Four-Leg Matrix Converter Ground Power Unit With Repetitive Voltage Control," *IEEE Transactions on Industrial Electronics (TIE)*, vol. 62, no. 4, pp. 2032-2040, April 2015.

[25] W.Rohouma, L.Empringham, P.Zanchetta, and P.Wheeler, "A four legs matrix converter based ground power unit with selective harmonic control," presented at *IEEE Energy Conversion Congress and Exposition (ECCE)*, 17-22 September 2011.

[26] R. Cardenas, R. Pena, P. Wheeler, and J. Clare, "Resonant Controllers for 4-leg Matrix Converters," presented at *IEEE International Symposium on Industrial Electronics* 4-7 July 2010.

[27] R. Cardenas, R. Pena, P. Wheeler, J. Clare, and G. Asher, "Control of the Reactive Power Supplied by a WECS Based on an Induction Generator Fed by a Matrix Converter," *IEEE Transactions on Industrial Electronics*, vol. 56, no. 2, pp. 429-438, February 2009.

[28] M. Vijayagopal, P. Zanchetta, L. Empringham, L. d. Lillo, L. Tarisciotti, and P. Wheeler, "Control of a Direct Matrix Converter With Modulated Model-Predictive Control," *IEEE Transactions on Industry Applications*, vol. 53, no. 3, pp. 2342-2349, May-June 2017.

[29] M. Rivera, J. Rodriguez, P. W. Wheeler, C. A. Rojas, A. Wilson, and J. R. Espinoza, "Control of a Matrix Converter With Imposed Sinusoidal Source Currents," *IEEE Transactions on Industrial Electronics*, vol. 59, no. 4, pp. 1939-1949, April 2012.

[30] J. Rodriguez, M. Rivera, J. W. Kolar, and P. W. Wheeler, "A Review of Control and Modulation Methods for Matrix Converters," *IEEE Transactions on Industrial Electronics*, vol. 59, no. 1, pp. 58-70.

[31] H. Abu-Rub, M. Malinowski, and K. Al-Haddad, "Power Electronics for Renewable Energy Systems, Transportation and Industrial Applications," John Wiley & Sons, 2014.

[32] S. Bhattacharya and D. Divan, "Synchronous frame based controller implementation for a hybrid series active filter system," presented at *Industry Applications Conference, Thirtieth IAS Annual Meeting*, 8-12 Oct. 1995.

[33] B. Singh and V. Verma, "Selective Compensation of Power-Quality Problems Through Active Power Filter by Current Decomposition," *IEEE Transactions on Power Delivery*, vol. 23, no. 2, pp. 792-799, April 2008.

[34] J. Rodriguez and P. Cortes, *Predictive Control of Power Converters and Electrical Drives.* vol. 37: Wiley, 2012.

[35] M. B. Shadmand, R. S. Balog, and H. Abu-Rub, "Auto-Tuning the Cost Function Weight Factors in a Model Predictive Controller for a Matrix Converter VAR Compensator," in *IEEE IEEE Energy Conversion Congress and Exposition (ECCE)*, Montreal, Canada, 20-24 Sept. 2015, pp. 3807 - 3814.

[36] P. Cortes, S. Kouro, B. La Rocca, R. Vargas, J. Rodriguez, J. I. Leon, S. Vazquez, and L. G. Franquelo, "Guidelines for weighting factors design in Model Predictive Control of power converters and drives," presented at *IEEE International Conference on Industrial Technology*, Feb. 2009.